Final Technical Report

Project Title

Geodetic Constraints on the Slip Rate of the Mohawk Valley Fault Zone, California

Award number: *08HQGR0027*

Principal Investigator & Contact Information:

Cornelis Kreemer
Nevada Bureau of Mines and Geology
University of Nevada, Reno
1664 N. Virginia Street, Reno, NV 89557
Tel: 775-682-8780; Fax: 775-784-1709

Co-Investigator:
William C. Hammond
Nevada Bureau of Mines and Geology
University of Nevada, Reno

Summary

The Mohawk Valley Fault Zone (MVFZ) is a seismically active, predominantly strike-slip, fault zone in the northern Walker Lane, California. We established 18 new GPS monuments across the MVFZ. These monuments are similar to all other monuments established by the Nevada Geodetic Laboratory in the area, some of which were already established in the study area. These sites have been occupied for at least three campaigns over >2 year time-span. Most campaigns were 1-2 months long. We analyzed all data for these sites as well as for the regional continuous GPS sites from EarthScope's Plate Boundary Observatory, and created position time-series from which we derived horizontal velocities. We rotated these velocities into a frame relative to the northern Sierra Nevada –Great Valley microplate by minimizing the velocities of 8 continuous stations. Velocities in this frame are predominantly oriented parallel to the trace MVFZ. We used the gradient of the along-strike velocities to infer a strike slip rate of 2.7±0.2 mm/yr (with a locking depth of 16.4±3.1 km). The normal rate is zero to within uncertainties. We will occupy all stations again in 2010, after which uncertainties in the velocities will be small enough to consider 1) any along-strike variation of slip, 2) a superimposed effect of other regional faults, 3) the possibility of unrecognized fault-normal component, and 4) the possible effect of asymmetry in crustal rigidity between the Sierra Nevada crust to the west and Sierra Valley to the east. Those results will feed into a peer-reviewed publication.

Report

Background

The Mohawk Valley Fault Zone (MVFZ) is located in the northern Walker Lane and likely marks the eastern boundary of the northern Sierra Nevada Mountains (Figure 1). The MVFZ is currently not directly used as input into the National Seismic Hazard Map (NSHM). This absence is, on one hand, understandable because of the dearth of paleoseismic data for this fault zone, but on the other is surprising given the relatively high seismicity rate along the MVFZ (Figure 2). Moreover, preliminary geodetic slip rates are relatively high compared to other faults in the Basin and Range (2-6 mm/yr) [*Dixon et al.*, 2000; *Hammond and Thatcher*, 2007]. We use the term MVFZ for the entire ~100 km long fault zone between roughly the town of Truckee and 40°N (south of Lake Almanor at northwest corner of Figure 1), where many faults and lineaments have been recognized [*Olig et al.*, 2005a]. The USGS Quaternary Fault and Fold database [*Haller et al.*, 2002; *Cao et al.*, 2003] only recognizes a small portion of it as the MVFZ and has it divided into the Mohawk Valley section (fault # 25a) and the Sierra Valley section (fault # 25b). The many late Quaternary faults and lineaments between Lake Tahoe and the southern tip of USGS fault 25b have been recognized and named as the Sierra Nevada fault zone [*Olig et al.*, 2005b] and renamed as the Truckee fault zone [*Olig et al.*, 2005a], but we consider it part of the MVFZ. The Grizzly Valley fault zone (trending ~55km NW from the town of Loyalton, parallel to the MVFZ) [*Briggs and Wesnousky*, 2003] may be distinct from the MVFZ, but further study is needed to understand their relative roles.

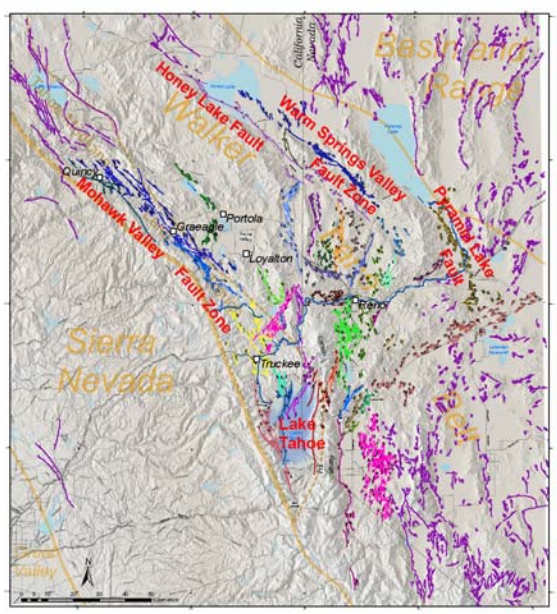

Fig. 1) *Quaternary fault compilation for a part of the northern Walker Lane, Sierra Nevada transition zone (modified after [Olig et al., 2005a]).*

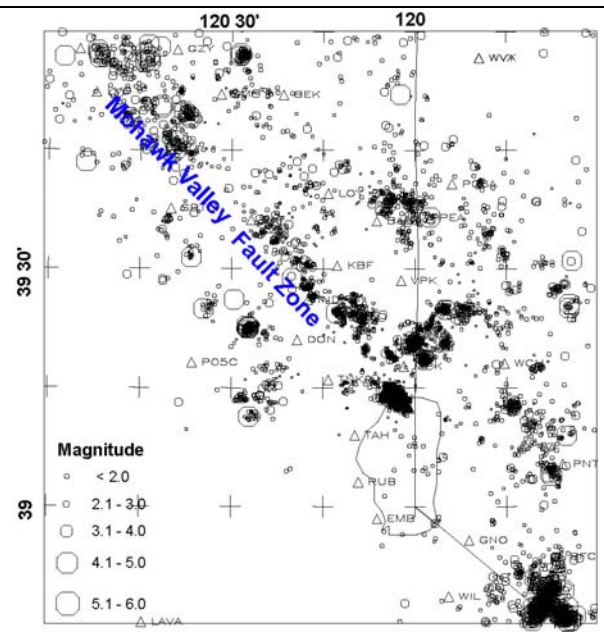

Fig. 2) *Epicenters from the Nevada Seismological Laboratory for events between 1986-2006. Locations of seismic stations are shown as well. The MVFZ is highlighted by the linear cluster of seismicity between the north end of Lake Tahoe and the northwest corner of the figure.*

Although not included in the current NSHM, the seismic source for the MVFZ has been characterized with a maximum preferred magnitude of M=7.3 [*Olig et al.*, 2005a], which does not include

the possibility of the rupture extending along their "Truckee fault zone" towards Truckee. If the entire fault zone ruptured in one earthquake, especially with a southward rupture directivity, an M=7.3+ event would be catastrophic for the town of Truckee, the rapidly expanding developments in Mohawk Valley, the town of Quincy, and the greater Reno-Carson City area. The two most important constraints in validating the likelihood of the occurrence of such an event come from better knowing the present-day slip rate and the extent of segmentation/connectedness along the fault zone. This geodetic study addresses the first issue. We limited our study to the part of the MVFZ between the towns of Truckee and Graeagle (in the Mohawk Valley), because this segment is likely representative of the MVFZ.

The high rate of micro-seismicity along the MVFZ (Figure 2, see also [*Rogers et al.,* 1991; *Goter et al.,* 1994]) is unusual for most faults in the Walker Lane, and may indicate that this fault is an important player in accommodating regional deformation between the Sierra Nevada/Great Valley and the Basin and Range. The epicenters from the Nevada Seismological Laboratory catalog suggest a heterogeneous distribution: diffuse NW of Sierra Valley, absent where the MTVZ bounds the southwestern Sierra Valley, and intermittently more concentrated between Sierra Valley and Truckee. In addition there is an apparent lineament of seismicity west and parallel to the MVFZ, in the Sierra Nevada mountains. Since 1960 there have been 30 M>4 events in the vicinity of the MVFZ, the largest of which is the 2001 Mw=5.2 Portola earthquake. The area between Verdi and Reno has also been unusually active, with at least 3 M>6 events over the last century [*dePolo et al.,* 1997]. Unusually deep and concentrated seismicity, comprising over 1600 events, occurred over several months in late 2003 underneath northern Lake Tahoe, likely related to a deep magmatic dyke intrusion [*Smith et al.,* 2004], and since then two M>4 events have happened near there. For most events along the MVFZ for which a focal mechanism has been determined the style is predominantly strike-slip with one nodal plane oriented sub-parallel to the strike of the MVFZ, indicating dextral offsets [*Ichinose et al.,* 2004].

There is very little available data or published discussion on the Quaternary activity of the MVFZ. One study [*Sawyer et al.,* 2003; , 2005] found that 2-3 Holocene events have ruptured a site in the southern Sierra Valley, with a recurrence interval of ~3,400 years, and an inferred right-lateral slip rate of 0.3-0.5 mm/yr. The segment closer to the Sierras appears to have predominantly normal slip, with a much longer recurrence interval, and a long-term vertical slip rate of 0.2-0.4 mm/yr [*Sawyer et al.,* 1993]. The paleoseismic investigations thus mark the MVFZ as a relatively slow oblique dextral fault zone, slower than inferred slip rates on other right-lateral faults in the northern Walker Lane: 1.1-2.3 mm/yr along the Honey Lake fault [*Wills and Borchardt,* 1993], 0.7-1.2 mm/yr (but possibly 2.2 mm/yr) on the Warm Springs Valley fault zone [*dePolo,* 2006], and up to 2.6±0.3 mm/yr along the Pyramid Lake fault [*Briggs and Wesnousky,* 2004]. The total slip rate across these three fault zones is consistent with the long-term slip rate inferred by [*Faulds et al.,* 2005].

Geodetic estimates of the total slip rate across the northern Walker Lane have varied from 6-8 mm/yr [*Thatcher et al.,* 1999] to 9.3 mm/yr [*Bennett et al.,* 2003] to ~10 mm/yr [*Kreemer et al.,* 2009]. The latter estimate is higher than the previous ones in part because it is based on GPS velocities that are corrected for the ongoing postseismic deformation following the historic earthquakes in the Central Nevada Seismic Belt which transfers some geodetic deformation further west into the Walker Lane [*Hammond et al.,* 2009]. The geodetic estimates for the slip rate on the MVFZ are much larger than the geologic rate estimates. These were first reported to be 6±3 mm/yr [*Dixon et al.,* 2000], but more recently [*Hammond and Thatcher,* 2007] reported a value of 2.3±0.3 mm/yr. The latter estimate was derived from a block-modeling approach in which the motion of crustal blocks, slip on the bounding faults, and the effect of elastic deformation due to fault coupling are simultaneously modeled. The slip rate estimate of [*Hammond and Thatcher,* 2007] for the MVFZ is the highest they found for any fault in the northern Walker Lane. However, their estimate was more uncertain than its formal error suggests, because of the sparse coverage of velocity estimates in the region and the related trade-off between the slip rate on the MVFZ and the Honey Lake fault.

Data Collection and Processing

The GPS data used in this project come from stations that can be placed in three different categories: a) continuously operating stations of EarthScope's Plate Boundary Observatory, b) UNR MAGNET stations that have been installed outside of this project, and c) UNR MAGNET stations that have been installed as part of this project. Data for all stations for with the time-series span >2 year of data have been used and the station distribution in the area of the MVFZ is shown in Figure 3.

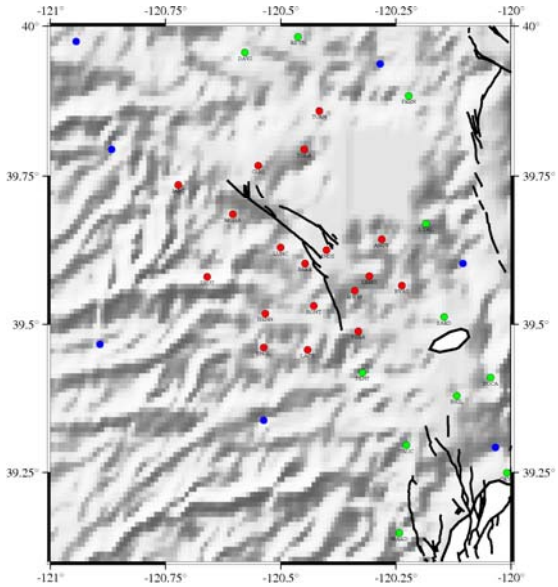

Fig. 3) *Red dots are MAGNET sites installed as part of this project, green dots are MAGNET sites installed outside this project, and blue dots are continuous PBO stations.*

Fig. 4) *Site LEMO in Lemon Valley, CA, installed as part of this project*

The UNR MAGNET monuments consist of a metal pin that is 7/8" wide and ~5" deep hole epoxyed into bedrock. An example of one of the sites in the study area is shown in Figure 4 and details on the monumentation and general observation strategy is given by *Blewitt et al.* [2009]. Data for the MAGNET stations are collected semi-continuously. This means that with having a fixed monument we simply place an antenna on the monument pin and attach it to a receiver (and power supply) at intermittent times. For each site we typically collect data for a few months per year (mostly in the summer months because of the snow, which covers most of this are between December-June).

Station coordinates were estimated every 24 hours using the precise point positioning method [*Zumberge et al.*, 1997]. Carrier phase ambiguities are successfully resolved across the entire network using an algorithm based on a fixed-point theorem that closely approximates a full-network resolution [*Blewitt*, 2008]. Satellite orbit and clock parameters, and daily coordinate transformation parameters into ITRF2005 were provided by the Jet Propulsion Laboratory (JPL). We included the latest satellite and receiver antenna phase center models. Ionosphere-free combinations of carrier phase and pseudorange were processed every 5 minutes. Estimated parameters included a tropospheric zenith bias and two gradient parameters estimated as random-walk processes, and station clocks estimated as a white-noise process. Formal errors for daily station positions were computed assuming 10-mm 1-standard deviation errors in the ionosphere-free carrier phase data. ITRF2005 positions were transformed into a North America fixed reference frame by performing daily transformations into a frame that is defined by minimizing the horizontal velocities of 11 stations across the stable part of the North America continent (away from areas affected by Glacial Isostatic Adjustments). Common mode errors on the continental scale are further reduced by including an additional 35 stations as far away as Greenland, Alaska, Hawaii, and the Caribbean in a daily spatial (7 parameter) filter.

We estimate velocities from the time-series using the CATS software package [see e.g.,*Williams*, 2003]. For the PBO stations and three MAGNET stations (BOCA, CRYS and WARD) we account for annual and semi-annual constituents. For the remaining site do we simply fit a constant velocity. The same software was used to estimates rate uncertainties given the assumption that the error model is dominated by white noise plus flicker noise. The time-series and best-fit motion model are shown in Figure 5 for all stations shown in Figure 3 with time-series >2 years.

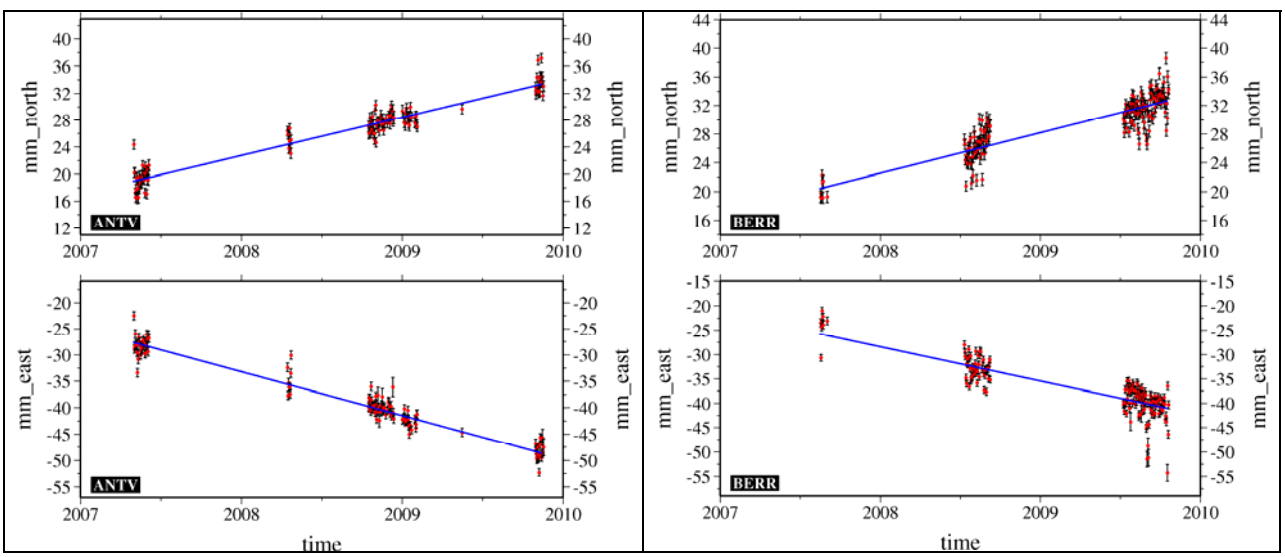

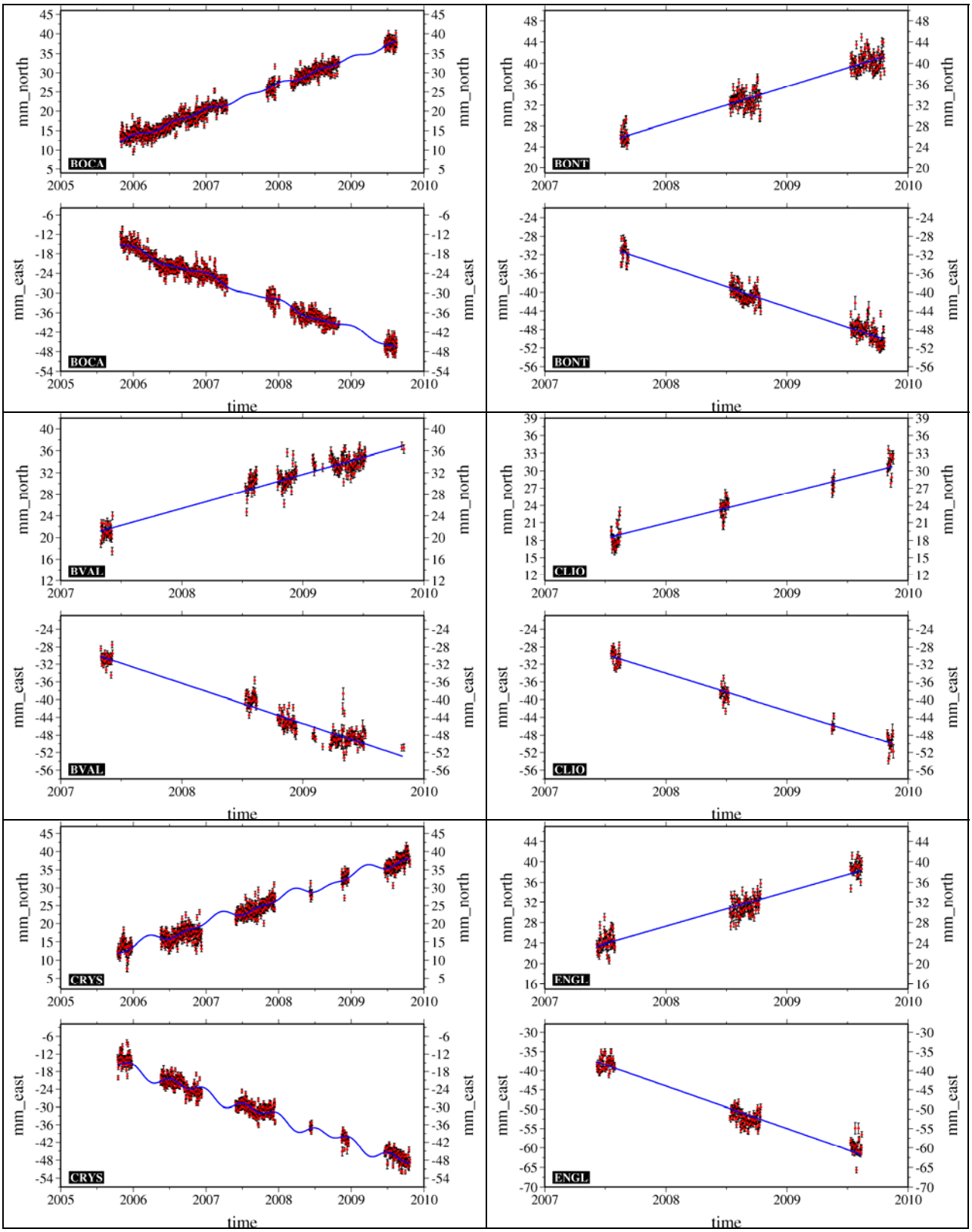
BOCA
BONT
BVAL
CLIO
CRYS
ENGL
mm_north
mm_east
time

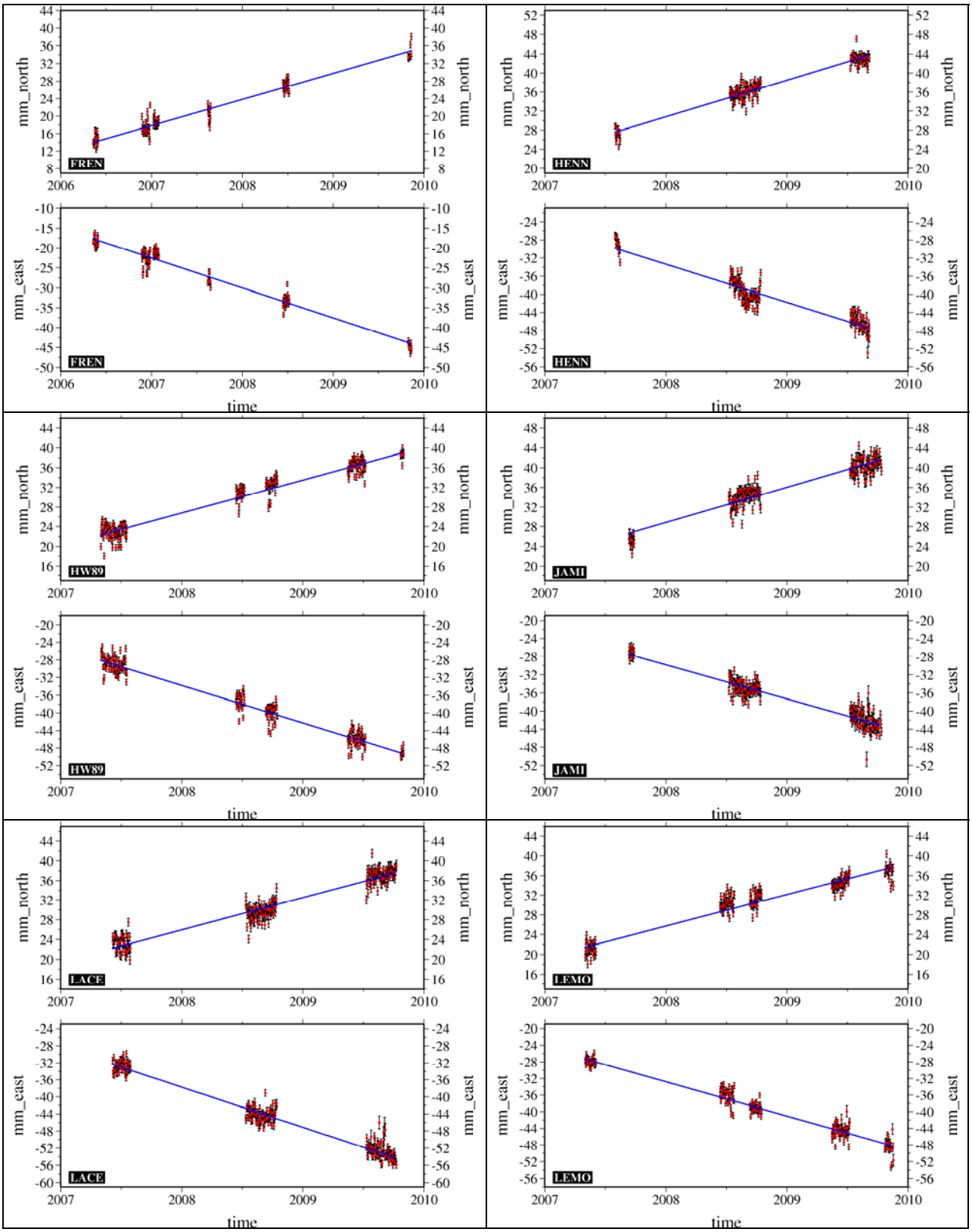
FREN
HENN
HW89
JAMI
LACE
LEMO
mm_north
mm_east
time

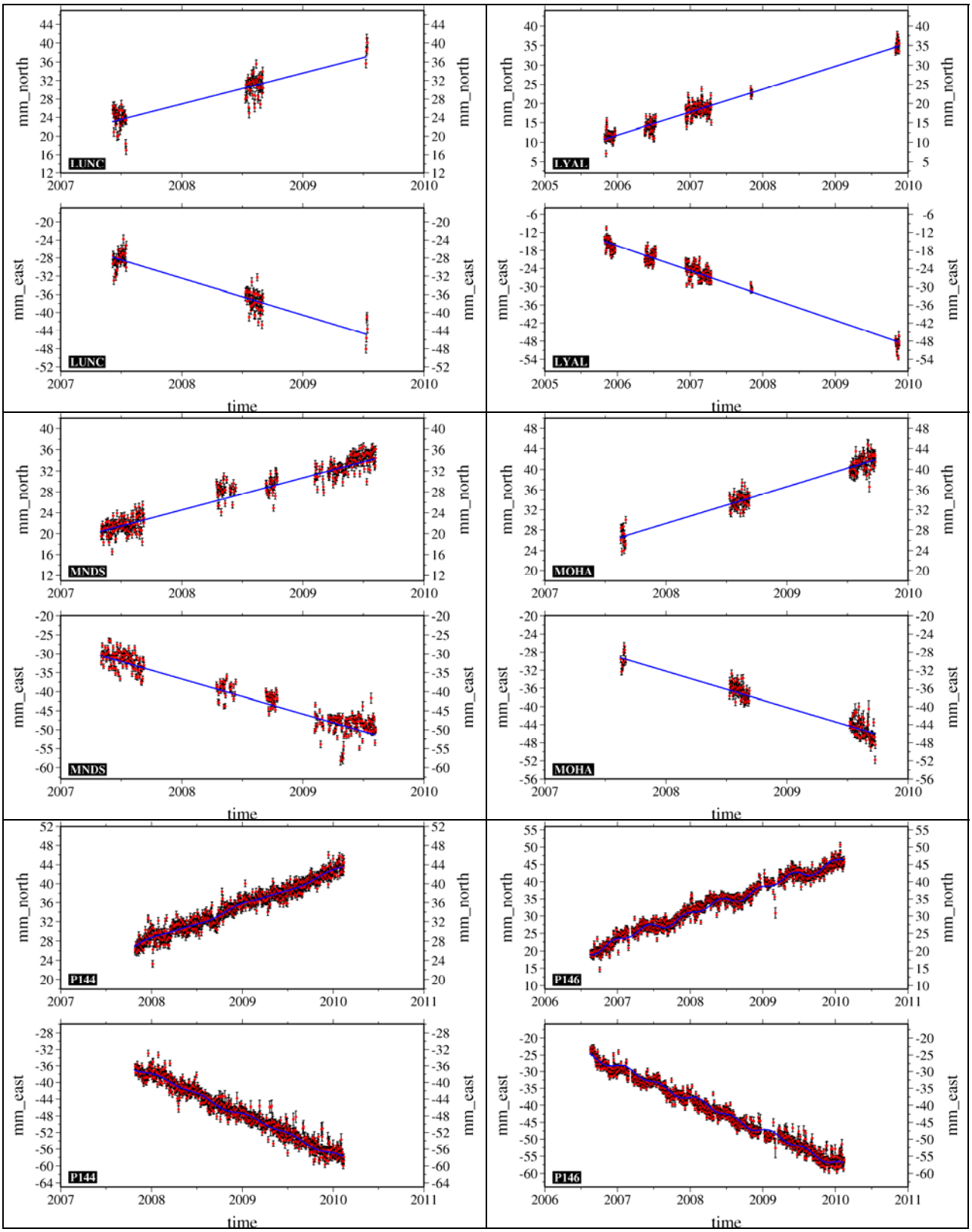
LUNC
LYAL
MNDS
MOHA
P144
P146
mm_north
mm_east
time

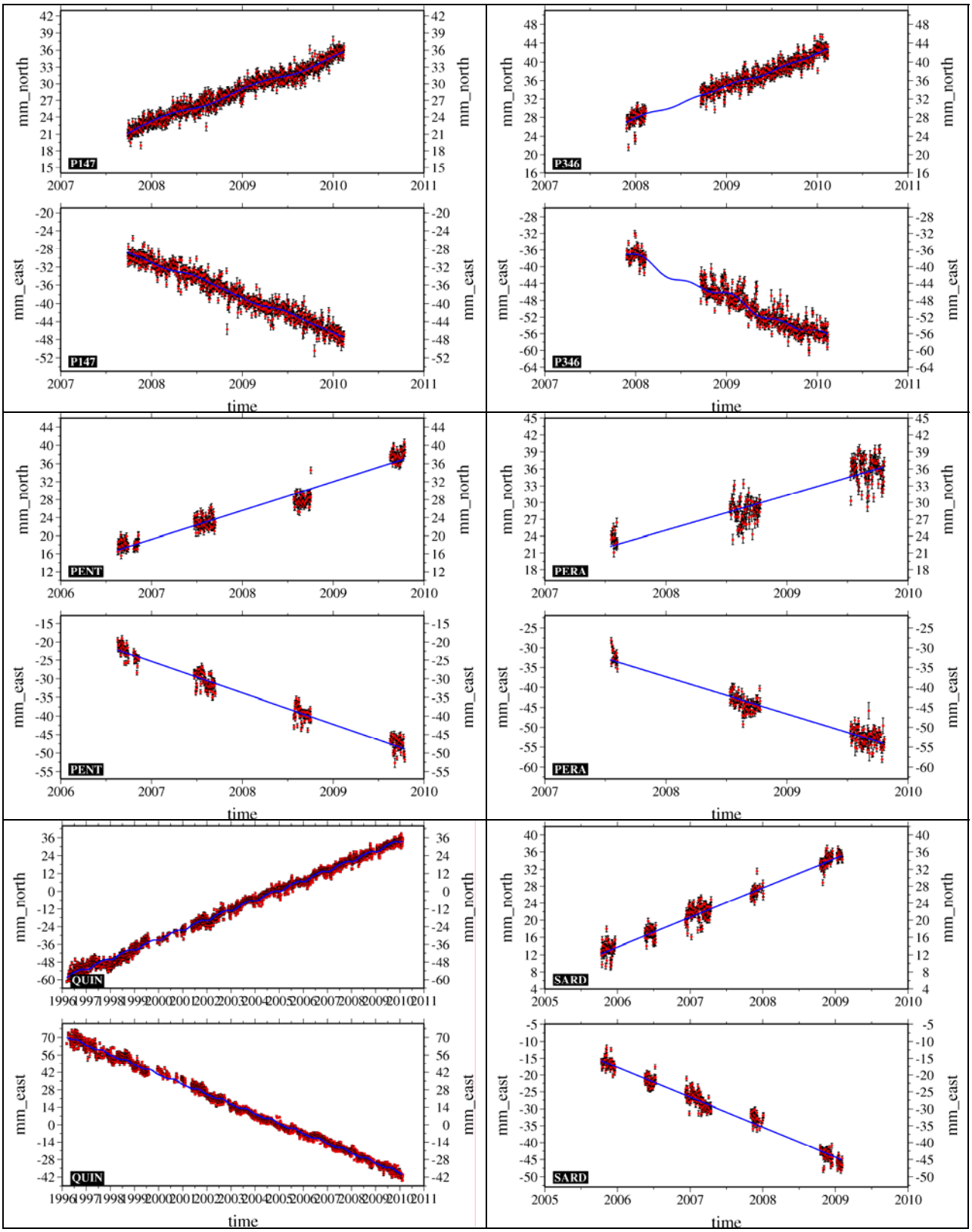
P147
P346
PENT
PERA
QUIN
SARD
mm_north
mm_east
time

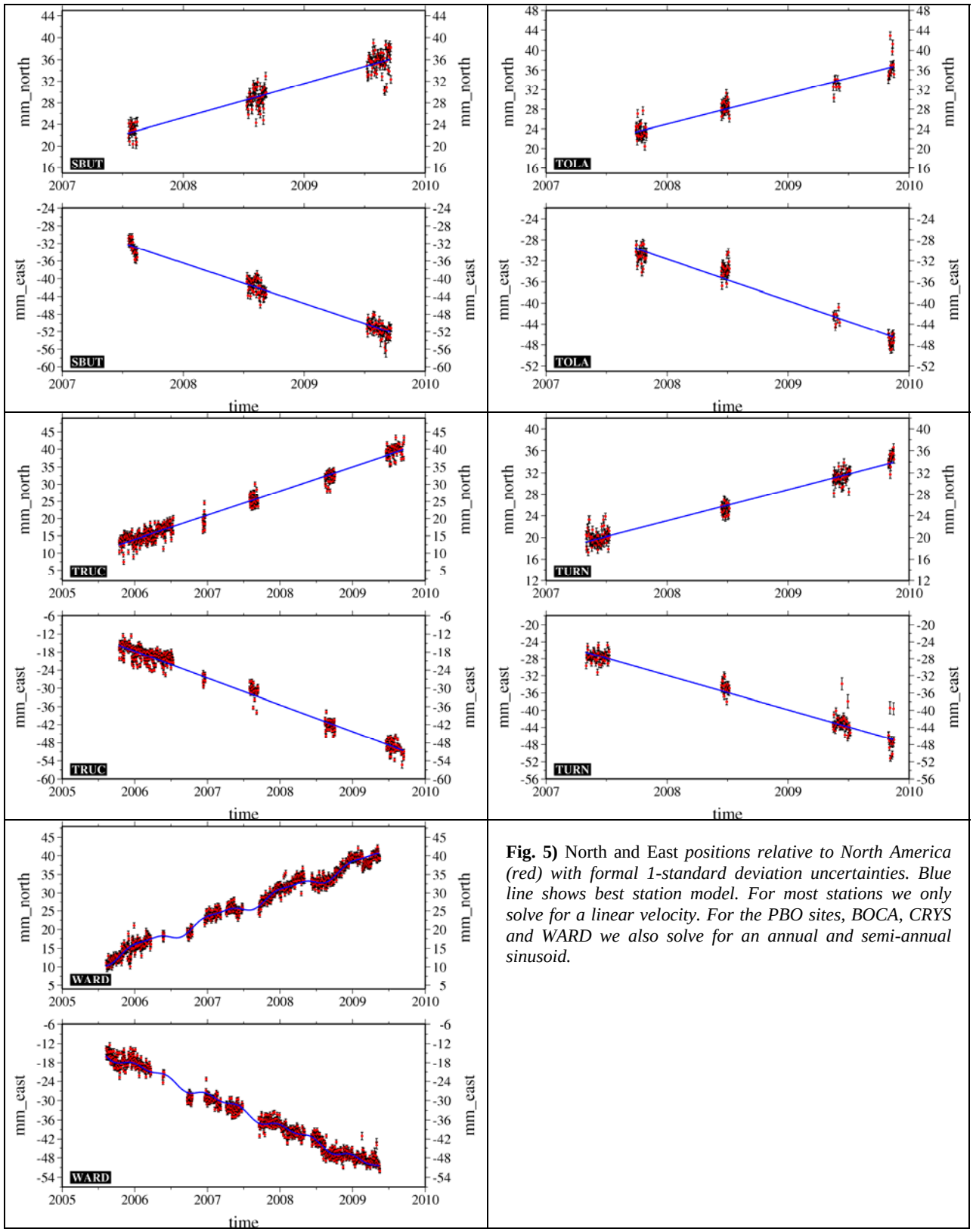

Fig. 5) North and East *positions relative to North America (red) with formal 1-standard deviation uncertainties. Blue line shows best station model. For most stations we only solve for a linear velocity. For the PBO sites, BOCA, CRYS and WARD we also solve for an annual and semi-annual sinusoid.*

Interpretation

To aid interpretation of the horizontal velocity gradient across the MVFZ we choose the place the velocities in a local reference frame defined by 8 sites on the northern Sierra Nevada - Great Valley (SNGV) microplate: ORVB, P140, P141, P146, P310, P339, SUTB, WARD. Velocities are tabulated in Table 1.

Table 1: GPS Velocities

station	Longitude (°E)	Latitude (°N)	*Period* start	*Period* end	*relative to North America* v_{east}	*relative to North America* v_{north}	*relative to North America* σ_{east}	*relative to North America* σ_{north}	*Northern SNGV* v_{east}	*Northern SNGV* v_{north}
ANTV	-120.281	39.643	2007.3	2009.9	-8.24	5.69	0.33	0.14	1.56	-1.73
BERR	-120.448	39.602	2007.6	2009.8	-8.25	5.91	1.23	0.66	1.57	-1.50
BOCA	-120.045	39.411	2005.8	2009.6	-8.41	6.53	0.36	0.27	1.39	-0.90
BONT	-120.428	39.531	2007.6	2009.8	-8.66	7.06	0.48	0.60	1.16	-0.35
BVAL	-120.237	39.565	2007.3	2009.8	-8.90	6.50	0.61	0.47	0.91	-0.92
CLIO	-120.549	39.768	2007.5	2009.9	-8.49	5.22	0.22	0.79	1.33	-2.18
CRYS	-120.010	39.249	2005.8	2009.8	-8.57	6.41	0.28	0.26	1.24	-1.02
ENGL	-120.537	39.462	2007.4	2009.6	-10.29	6.93	0.69	0.37	-0.46	-0.47
FREN	-120.222	39.884	2006.4	2009.9	-7.60	5.87	0.51	0.24	2.18	-1.55
HENN	-120.534	39.518	2007.6	2009.7	-9.16	7.81	0.87	0.33	0.67	0.40
HW89	-120.340	39.556	2007.3	2009.8	-8.44	6.56	0.16	0.32	1.37	-0.85
JAMI	-120.723	39.735	2007.7	2009.8	-7.64	7.72	0.40	0.56	2.19	0.33
LACE	-120.442	39.458	2007.4	2009.8	-9.25	6.31	0.47	0.39	0.57	-1.10
LEMO	-120.308	39.581	2007.3	2009.9	-7.99	7.02	0.47	0.58	1.82	-0.40
LUNC	-120.501	39.629	2007.4	2009.5	-7.68	6.72	0.69	0.34	2.14	-0.68
LYAL	-120.185	39.669	2005.8	2009.9	-8.28	5.85	0.38	0.34	1.51	-1.57
MNDS	-120.401	39.625	2007.3	2009.6	-8.14	6.65	1.35	0.71	1.67	-0.76
MOHA	-120.604	39.684	2007.6	2009.7	-7.53	7.31	0.65	0.17	2.30	-0.09
ORVB*	-121.500	39.555	1996.9	2010.1	-9.73	7.08	0.09	0.08	0.17	-0.27
P140*	-120.693	38.829	2006.5	2010.1	-9.55	7.72	0.19	0.16	0.34	0.33
P141*	-120.386	39.047	2006.8	2010.1	-9.79	7.67	0.54	0.46	0.06	0.25
P144	-120.893	39.467	2007.8	2010.1	-9.48	7.28	0.35	0.38	0.39	-0.10
P146*	-120.537	39.337	2006.6	2010.1	-9.67	7.53	0.74	0.67	0.18	0.12
P147	-120.284	39.937	2007.7	2010.1	-7.65	5.85	0.26	0.20	2.13	-1.57
P310*	-120.334	38.736	2006.6	2010.1	-9.54	7.60	0.23	0.28	0.33	0.18
P339*	-122.668	40.034	2007.3	2010.1	-9.56	7.14	0.34	0.34	0.41	-0.14
P346	-120.867	39.795	2007.9	2010.1	-9.00	7.04	1.00	0.55	0.84	-0.35
PENT	-120.323	39.419	2006.6	2009.8	-8.76	6.42	0.56	0.35	1.05	-0.99
PERA	-120.332	39.488	2007.5	2009.8	-9.75	5.68	0.48	0.71	0.06	-1.74
QUIN	-120.944	39.975	1996.2	2010.1	-8.47	6.73	0.22	0.34	1.36	-0.65
SARD	-120.146	39.513	2005.8	2009.1	-8.78	6.88	0.36	0.12	1.02	-0.55
SBUT	-120.660	39.580	2007.5	2009.7	-9.35	6.32	0.53	0.19	0.49	-1.08
SUTB*	-121.821	39.206	1997.2	2010.1	-10.21	7.58	0.08	0.09	-0.25	0.25
TOLA	-120.449	39.795	2007.7	2009.9	-7.83	6.28	0.55	0.22	1.97	-1.13
TRUC	-120.228	39.296	2005.8	2009.7	-8.83	7.01	0.41	0.32	0.99	-0.41
TURN	-120.417	39.859	2007.3	2009.9	-7.84	5.79	0.27	0.26	1.95	-1.62
WARD*	-120.243	39.148	2005.6	2009.4	-9.77	7.30	0.30	0.26	0.06	-0.12

Velocities and uncertainties are in mm/yr
* These stations are used to constrain the northern Sierra Nevada – Great Valley (SNGV) reference frame

Velocities relative to the northern SNGV are shown in Figure 6. The velocities are superimposed on top of the basemap of *Olig et al.* [2005a].

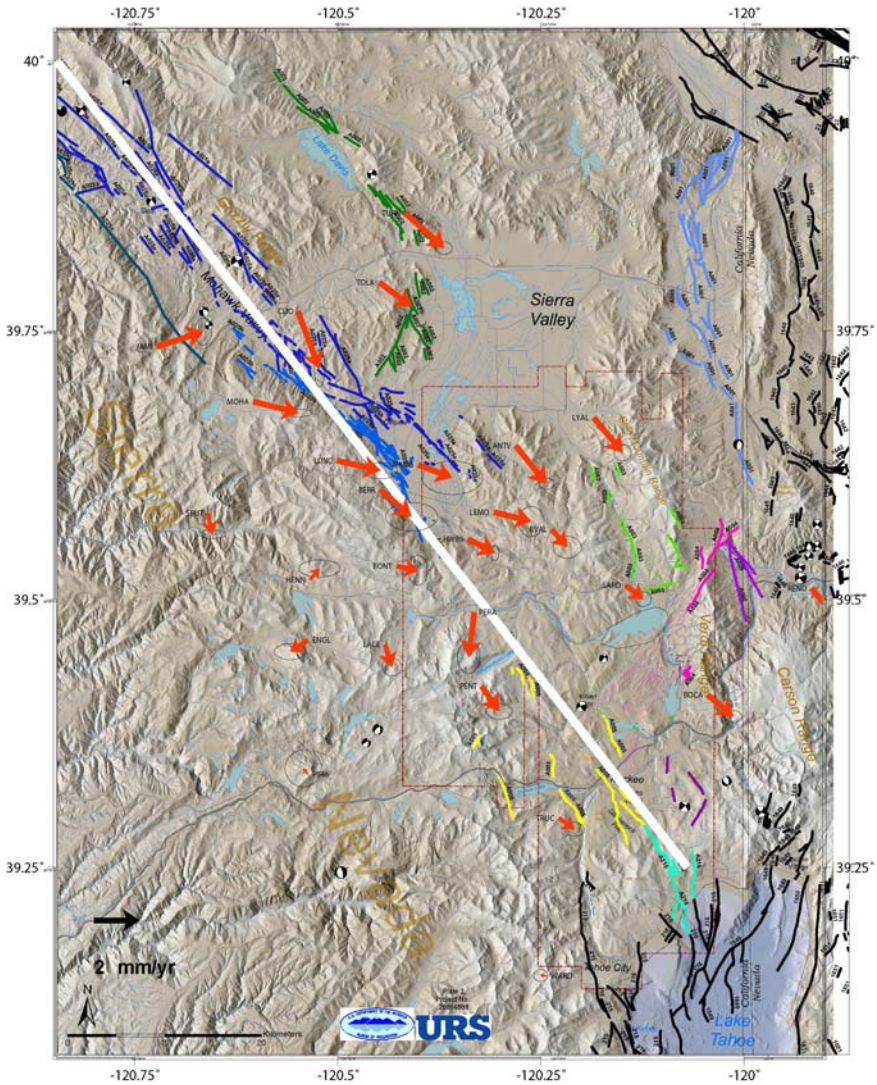

Fig. 6) *Orange vectors are velocities relative to the northern SNGV. Error ellipses represent 1-standard deviation uncertainties. Results are superimposed on basemap of* Olig et al. *[2005a]. Also shown are focal mechanisms of significant regional earthquakes. White line is the trace of the hypothetical single fault in an elastic half-space used to model the slip rate.*

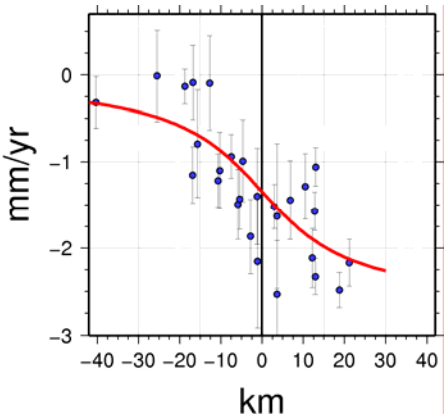

Fig. 7) *Velocity components parallel to the simplified MVFZ trace (Fig. 6) shown by blue circles with 1-standard deviation uncertainties. Predicted model (with slip rate of 2.7 mm/yr and seismogenic thickness of 16.4 km) is shown by red line.*

Velocities are mostly aligned in the same directions of the MVFZ and we therefore model the slip rate of the MHVZ as a vertical strike-slip fault in an elastic half-space. When we fix the trace to that shown on Figure 6 and take the fault-parallel component of the velocity field, we solve for a slip rate *s* and locking depth *d* and find *s*=2.7±0.2 mm/yr and *d*=16.4±1.9 km. The χ^2 per degree of freedom is 1.9. The fit to the data is shown in the cross-section shown in Figure 7.

Most of the velocities are from time-series less than 2.5 years, so velocity uncertainties are correspondingly large. As a result, the large uncertainties do not allow us yet to evaluate 1) along-strike variation of slip, 2) possible contribution from other regional faults (e.g., Honey Lake fault), 3) the possibility of a fault-normal component, and 4) the possible effect of asymmetry in crustal rigidity between the Sierra Nevada crust to the west and Sierra Valley to the east. Nevertheless, we present two alternative models. In the first, we solve for the location of the fault *X* while solving for *s* and *d*, and we find that *X*=-8.1±2.1 km, *s*=2.2±0.2mm/yr and *d*=8.1±2.9 km. The reduced χ^2 for this case is 1.8. The fit is shown in Figure 8a. This may not be a realistic model, since it places the fault traces clearly away from observed faults and seismicity. In the second alternative model we keep the fault trace fixed and assume a locking depth of 23 km, the maximum depth of seismicity in the area as recorded by the Nevada Seismologic Laboratory. We find that *s*=2.8±0.1mm/yr and the reduced χ^2 for this case is 2.0. Thus the slip rate is not very sensitive to the locking depth. The fit is shown in Figure 8b.

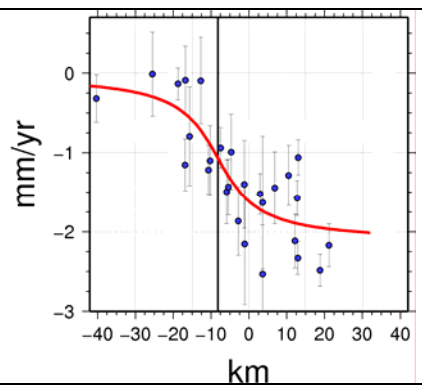

Fig. 8a) *Same as Fig 7, except that the location fault was solved for*

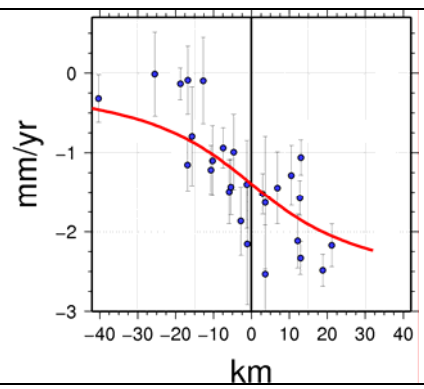

Fig. 8a) *Same as Fig 7, except that the seismogenic thickness is fixed to 23 km.*

Papers and Presentations

Briggs, R.W. and Hammond, W.C. (2009) Integration of geodetic and geologic data in the National Seismic Hazard Maps, report on workshop on geodetic and geologic datasets in the Northern Walker Lane, Reno Nevada, 21-22 April 2009, Eos, v. 90, no. 38, 22 Sept. 2009.

Hammond, W.C., Blewitt, G., Kreemer, C. (2010) Block modeling of crustal deformation of the northern Walker Lane and Basin and Range from the MAGNET GPS velocities, *J. Geophys. Res.*, in preparation.

Hammond et al., (2010) Block Models of Walker Lane and Great Basin tectonic deformation, slip rates and seismic cycle effects, talk and poster presented at SCEC Workshop on Incorporating Geodetic Surface Deformation Data into UCERF3, Pomona, CA, April 1-2.

Hammond et al. (2010) Highlights of geodetic measurement of the rifting of continental lithosphere in the Walker Lane, Western Great Basin, United States, MARGINS Successor Workshop, San Antonio, TX, Feb. 15-18

Hammond, W.C., Kreemer, C., Blewitt, G., New geodetic constraints on the location and style of eastern and northern Sierra Nevada crustal deformation, AEG Annual Meeting, , South Lake Tahoe, NV, September 21-26, 2009

Hammond, W.C., Kreemer, C., and Blewitt, G. (2009) Strain partitioning in the northern Walker Lane and western Basin and Range from GPS measurements, Eos Trans. AGU, 90(22) AGU Joint Assembly, Abstract G12A-06, May 24-27.

Kreemer, C., Hammond, W.C., and Blewitt, G. (2009), Geodetic constraints on the rigidity and eastern boundary of the Sierra Nevada micro-plate, from Mohawk Valley to Southern Walker Lane, *Eos Trans. AGU, 90(53), Fall Meet. Suppl., Abstract G23D-06*.

Kreemer, C., Hammond, W.C., and Blewitt, G. (2010), The slip rate of the Mohawk Valley Fault Zone, California, from GPS measurements, *Geophysical Research Letters*, in preparation.

Kreemer, C. (2009) Regional strain rate maps in northwestern Nevada, Geodesy/Geology Workshop, USGS, Reno, NV, April 21-22.

Kreemer, C. (2010) New GPS constraints on deformation in the Intermountain West, U.S. Geological Survey, CO, March 25.

Bibliography

Bennett, R. A., B. P. Wernicke, N. A. Niemi, A. M. Friedrich, and J. L. Davis (2003), Contemporary strain rates in the northern Basin and Range province from GPS data, *Tectonics, 22, 1008, doi:10.1029/2001TC001355*.

Blewitt, G. (2008), Fixed-point theorems of GPS carrier phase ambiguity resolution and their application to massive network processing: "Ambizap", *J. Geophys. Res., 113, B12410, doi:10.1029/2008JB005736*.

Blewitt, G., W. C. Hammond, and C. Kreemer (2009), Geodetic constraints on contemporary deformation in the northern Walker Lane: 1. Semi-permanent GPS strategy, in *Late Cenozoic Structure and Evolution of the Great Basin - Sierra Nevada Transition, GSA Special Volume 447*, edited by J. S. Oldow and P. Cashman, pp. 1-15, Geological Society of America, Boulder.

Briggs, R. W., and S. G. Wesnousky (2003), The role of the Grizzly Valley Fault Zone in accommodating shear of the northern Walker Lane, NE California, USA, *Geological Society of America Abstracts with Programs, 35*, 581.

Briggs, R. W., and S. G. Wesnousky (2004), Late Pleistocene fault slip rate, earthquake recurrence, and recency of slip along the Pyramid Lake fault zone, northern Walker Lane, United States, *J. Geophys. Res., 109, B08402, doi:10.1029/2003JB002717*.

Cao, T., W. A. Bryant, B. Rowshandel, D. Branum, and C. J. Wills (2003), The revised 2002 California probabilistic seismic hazard maps, Open-File Report 96-08, U.S.G.S.

dePolo, C. M. (2006), Determination of fault slip rates, plaeoearthquake history, and segmentation of the Warm Springs Vally Fault System, Final Technical Report, National Earthquake Hazards Reduction Program, Grant 04HQGR0082, 35 pp.

dePolo, C. M., J. G. Anderson, D. M. dePolo, and J. G. Price (1997), Earthquake occurence in the Reno-Carson City urban corridor, *Seismological Research Letters, 68*, 401-412.

Dixon, T. H., M. Miller, F. Farina, H. Z. Wang, and D. Johnson (2000), Present-day motion of the Sierra Nevada block and some tectonic implications for the Basin and Range province, North American Cordillera, *Tectonics, 19*, 1-24.

Faulds, J. E., C. D. Henry, and N. H. Hinz (2005), Kinematics of the northern Walker Lane: An incipient transform fault along the Pacific-North American plate boundary, *Geology, 33*, 505-508.

Goter, S. K., D. H. Oppenheimer, J. J. Mori, M. K. Savage, and R. P. Masse (1994), Earthquakes in California and Nevada, Open-File Report 94-647, U.S. Geological Survey.

Haller, K. M., R. L. Wheeler, and K. S. Rukstales (2002), Documentation of changes in fault parameters for the 2002 National Seismic Hazard Maps - Conterminous United

States except California, Open-File Report 02-467, U.S.G.S.

Hammond, W. C., and W. Thatcher (2007), Crustal deformation across the Sierra Nevada, Northern Walker Lane, Basin and Range transition, Western United States, measured with GPS, 2000-2004, *J. Geophys. Res.*, *112, B05411, doi:10.1029/2006JB004625*.

Hammond, W. C., C. Kreemer, and G. Blewitt (2009), Geodetic constraints on contemporary deformation in the northern Walker Lane: 3. Postseismic relaxation in the Central Nevada Seismic Belt, in *Late Cenozoic Structure and Evolution of the Great Basin - Sierra Nevada Transition, GSA Special Volume 447*, edited by J. S. Oldow and P. Cashman, pp. 33-54, Geological Society of America, Boulder.

Ichinose, G. A., J. G. Anderson, K. D. Smith, and Y. H. Zeng (2004), Source parameters of eastern California and western Nevada earthquakes from regional moment tensor inversion, *Bull. Seism. Soc. Am.*, *93*, 61-84.

Kreemer, C., G. Blewitt, and W. C. Hammond (2009), Geodetic constraints on contemporary deformation in the northern Walker Lane: 2. Velocity and strain rate tensor analysis, in *Late Cenozoic Structure and Evolution of the Great Basin - Sierra Nevada Transition, GSA Special Volume 447*, edited by J. S. Oldow and P. Cashman, pp. 17-31, Geological Society of America, Boulder.

Olig, S., T. Sawyer, D. Wright, F. Terra, and L. Anderson (2005a), Preliminary seismic source characterization of faults near Stampede and Prosse Creek dams - Washoe project and Boca Dam - Truckee storage project, 65 pp, U.S. Department of the Interior, Bureau of Reclamation, Denver.

Olig, S., T. Sawyer, L. Anderson, D. Wright, I. Wong, and F. Terra (2005b), Insights into Quaternary strain patterns in the northern Walker Lane from mapping and source characterization of faults near Truckee, California, *Seismological Research Letters*, *76*, 251.

Rogers, A. M., S. C. Harmsen, E. J. Corbett, K. Priestley, and D. dePolo (1991), The seismicity of Nevada and some adjacent parts of the Great Basin, in *Neotectonics of North America: Geological Society of America, Decade Map Volume*, edited by D. B. Slemmons, et al., pp. 153-184.

Sawyer, T. L., W. D. Page, and M. A. Hemphill-Haley (1993), Recurrent late Quaternary surface faulting along the Mohawk Valley fault zone, NE California, *Geological Society of America, Abstracts with Programs*, *25*, 142.

Sawyer, T. L., R. W. Briggs, and A. R. Ramelli (2003), Paleoseismic investigations of the Mohawk Valley fault zone, Sierra County, northeastern California, Annual Project Summary, U.S. Geological Survey National Earthquake Hazards Reduction Program, Award 04HQGR0089, 4 pp.

Sawyer, T. L., R. W. Briggs, and A. R. Ramelli (2005), Late Quaternary activity of the southern Mohawk Valley fault zone, northeastern California, *Seismological Research Letters*, *76*, 248.

Smith, K. D., D. von Seggern, G. Blewitt, L. Preston, J. G. Anderson, B. P. Wernicke, and J. L. Davis (2004), Evidence for deep magma injection beneath Lake Tahoe, Nevada-California, *Science*, *305*, 1277-1280.

Thatcher, W., G. R. Foulger, B. R. Julian, J. Svarc, E. Quilty, and G. W. Bawden (1999), Present-day deformation across the basin and range province, western United States, *Science*, *283*, 1714-1718.

Williams, S. D. P. (2003), The effect of coloured noise on the uncertainties of rates estimated from geodetic time series, *J. Geodesy*, *76*, 483-494.

Wills, C. J., and G. Borchardt (1993), Holocene slip rate and earthquake recurrence on the Honey Lake fault zone, *Geology*, *21*, 853-856.

Zumberge, J. F., M. B. Heflin, D. C. Jefferson, M. M. Watkins, and F. H. Webb (1997), Precise point positioning for the efficient and robust analysis of GPS data from large networks, *J. Geophys. Res.*, *102*, 5005-5017.